JOURNAL OF MATERIALS SCIENCE 35 (2000) 2937–2948

# Predicting times to low strain for a 1CrMoV rotor steel using a 6-$\theta$ projection technique

M. EVANS
*Department of Materials Engineering, University of Wales Swansea, Singleton Park, Swansea, UK, SA2 8PP*
*E-mail: m.evans@swansea.ac.uk*

The $\theta$ projection method of creep analysis is known to produce the poorest predictions of creep properties at low strains. This paper applies a recently suggested modification of the $\theta$ concept to 1CrMoV rotor steel where long term data exists to enable an assessment of this modification to be made. The modification takes the form of two additional $\theta$ terms that allow the initial stages of any creep curve to be modelled more accurately. The paper shows that the resulting 6-$\theta$ approach produces predictions of long-term failure times and minimum creep rates that are as good as those obtained using the traditional 4-$\theta$ approach. Unlike the 4-$\theta$ approach, the 6-$\theta$ approach is also shown to be capable of accurately predicting times to very low strains (0.05% and 0.1%) at stress levels as low as 77 MPa (well below the lowest stress of 230 MPa used in the theta analysis). For times to 1.0% strain or more the 4-$\theta$ and 6-$\theta$ techniques give similar short and long-term predictions.


## 1. Introduction

When designing materials for high temperature service the design criteria for long term operation must guarantee that creep deformation should not cause excessive distortion over the planned service life and that creep failure should not occur within such a required operating life. Such creep fracture represents an obvious 'life limiting' design consideration as fracture of pipework or other major components used by nuclear powered electricity generating plants could prove catastrophic. For this reason, studying their ability to predict the time to rupture strain has been the major criteria used to assess creep extrapolation techniques. However, substantial problems can also be encountered due to excessive creep distortion. There are numerous examples of such deformation limits within the power generation and aero engine industries. For example, the blades of a steam turbine cannot be allowed to extend until they foul the surrounding casting. Similar requirements exist for the blades used in a gas turbine aeroengine.

The $\theta$ projection technique [1, 2] is ideally suited to the prediction of times to various low strains rather than just times to rupture strain. Traditional parametric procedures (such as the Larson-Miller technique [3]) are not considered here because they are limited to the prediction of times to rupture strain. In contrast, the $\theta$ methodology allows the whole creep curve to be extrapolated to design (low) stresses from accelerated stresses. Time to any strain can then be 'read off' from such extrapolated creep curves.

The 1CrMoV rotor steel data set published by Evans *et al.* [4] will be used to study the predictions made of time to various low strains using the $\theta$ projection concept. Whilst Evans *et al.* have already assessed the ability of the $\theta$ projection technique to extrapolate minimum creep rates and failure times from this accelerated test data, they have not assessed its ability to predict low strain times. This paper addresses this shortcoming and then goes on to show how the $\theta$ prediction technique can be modified along the lines recently suggested by Evans [5] to improve such low strain time predictions.

This paper is therefore structured as follows. First, the experimental procedure and database are discussed. The following section then briefly reviews the $\theta$ methodology so that key differences between the traditional 4-$\theta$ concept and the new 6-$\theta$ concept become clear. Section 4 compares and contrasts the 4-$\theta$ and 6-$\theta$ creep curves obtained under the accelerated test conditions. Section 5 then assesses the accuracy of the long-term predictions made for the minimum creep rate, time to rupture strain and time to various low strains using the 4-$\theta$ and 6-$\theta$ techniques. A final section concludes.

## 2. Experimental procedures

The batch of material used for the present investigation represents the lower bound creep strength properties anticipated for 1CrMoV rotor steels. The chemical composition of this batch of material (in wt %) was determined as 0.27%C, 0.22%Si, 0.77%Mn, 0.008%S, 0.015%P, 0.97%Cr, 0.76%Ni, 0.85%Mo, 0.39%V, 0.125%Cu, 0.008%Al and 0.017%Sn. Following oil quenching from 1238 K and tempering at 973 K, the material had a tensile strength of 741 MPa, elongation of 17%, reduction in area of 55% and a 0.2% proof stress of 618 MPa.

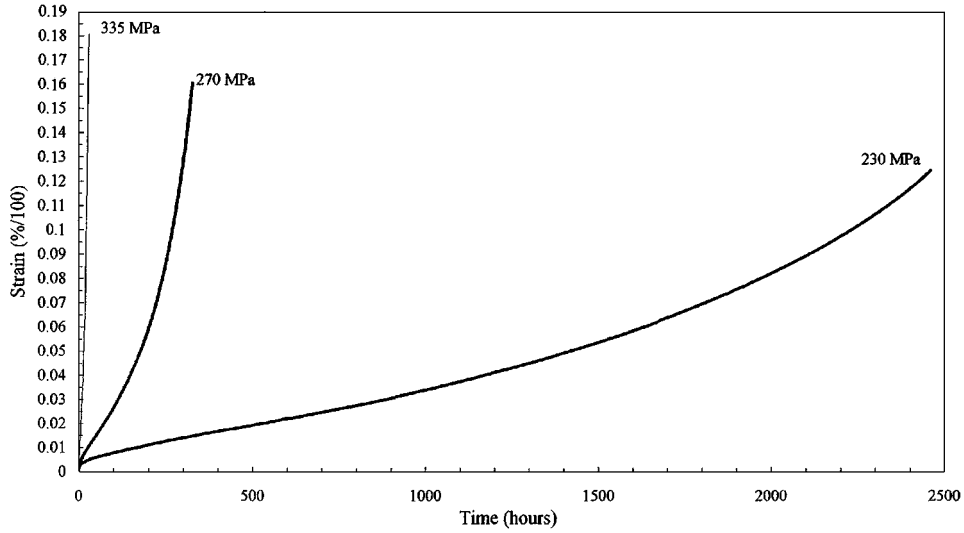


*Figure 1* Constant stress creep curves recorded for 1CrMoV rotor steel in tests carried out at 823 K. The solid lines represent smoothing through the creep strain/time recordings.

Nineteen test pieces, with a gauge length of 25.4 mm and a diameter of 3.8 mm, were tested in tension over a range of stresses at 783 K, 823 K and 863 K using high precision constant-stress machines [6]. At 783 K, six specimens were placed on test over the stress range 425 MPa to 290 MPa, at 823 K seven specimens were placed on test over the stress range 335 MPa to 230 MPa and at 863 K six specimens were tested over the stress range 250 MPa to 165 MPa. Up to 400 creep strain/time readings were taken during each of these tests. Normal creep curves were observed under all these test conditions, as illustrated in Fig. 1.

These nineteen specimens represent the accelerated test data to which various $\theta$ projection techniques will be applied below. To assess the extrapolative capability of these techniques long-term property data was supplied independently by an industrial consortium involving GEC-Alsthom, Babcocks Energy, National Power, PowerGen and Nuclear Electric. These long-term properties came from the same batch of material used in the accelerated test programme described above but for specimens with gauge lengths of 125 mm and diameters of 14 mm that were subjected to tests on high sensitivity constant-load tensile creep machines. It is important to note that in all cases below the $\theta$ projection techniques did not make use of this long-term property data. The $\theta$ techniques used only the accelerated test data to predict the properties of these longer-term test results.

## 3. The $\theta$ projection concept: Old and new

### 3.1. The technique

The 4-$\theta$ technique describes the shape of any creep curve displaying normal primary and tertiary stages by using four theta parameters through the equation

$$\varepsilon_t = \theta_1(1 - e^{-\theta_2 t}) + \theta_3(e^{\theta_4 t} - 1) \qquad (1)$$

where $\varepsilon_t$ is the creep strain recorded at time $t$ (with $n$ such recordings in total). In Equation 1, $\theta_1$ quantifies the total primary strain, $\theta_2$ the curvature of the creep curve during primary creep, $\theta_3$ scales the tertiary creep strain and $\theta_4$ measures the curvature of the creep curve during tertiary creep.

The idea is then to test various specimens at accelerated stresses ($\sigma_j$) and temperatures ($T_j$) and then to fit Equation 1, using non linear optimisation techniques (see Section 3.2 below), to each of the resulting creep curves. Each $\theta_i$ ($i = 1$ to 4) is then related to the accelerated test conditions through a simple 'linear' expression of the form

$$L[\theta_{ij}] = \beta_{i0} + \beta_{i1}\sigma_j + \beta_{i2}T_j + \beta_{i3}\sigma_j T_j \qquad (2)$$

where $\sigma_j$ is the stress associated with test condition $j$ and $T_j$ the temperature associated with test condition $j$ ($j = 1$ to $m$). $\beta_{i0}$ to $\beta_{i3}$ are constants that can be estimated using linear least squares. Alternatively, weighted least squares can be used to reflect the fact that each $\theta_{ij}$ value is only an estimate of its true value. The weights used must reflect the different uncertainties associated with each $\theta_{ij}$. Each $\theta_i$ can then be extrapolated to lower stresses and temperatures by simply substituting the required test conditions into Equation 2. Let $\tilde{\theta}_{ij}$ represents such extrapolated theta values. It is now possible to use these values to predict a variety of creep properties at close to the operating conditions for a designed material. For example, a prediction of the minimum creep rate at condition $j$ can be found by substituting

$$t_M = \frac{1}{\tilde{\theta}_{2j} + \tilde{\theta}_{4j}} \ln \frac{\tilde{\theta}_{1j}\,\tilde{\theta}_{2j}^2}{\tilde{\theta}_{3j}\,\tilde{\theta}_{4j}^2} \qquad (3)$$

for $t$ and $\tilde{\theta}_{ij}$ for $\theta_i$ into

$$\dot{\varepsilon}_t = \theta_1\theta_2 e^{-\theta_2 t} + \theta_3\theta_4 e^{\theta_4 t} \qquad (4)$$

where $\dot{\varepsilon}_t$ is the creep rate at time $t$. Similarly, a prediction of the time to reach some specified creep strain, $\varepsilon^*$, can be obtained by solving numerically for time in the equation

$$\tilde{\theta}_{1j}(1 - e^{-\tilde{\theta}_{2j} t}) + \tilde{\theta}_{3j}(e^{\tilde{\theta}_{4j} t} - 1) - \varepsilon^* = 0. \qquad (5)$$

As a special case of this, the failure time $t_F$ can be predicted by solving Equation 5 when $\varepsilon^*$ equals the rupture strain. Of course this requires the rupture strain to be extrapolated to the required conditions as well. This is typical done using a formula similar to Equation 2 (i.e. replace $\theta_{ij}$ with $\varepsilon_j^F$ where $\varepsilon_j^F$ is the rupture strain observed at the accelerated test conditions).

A number of factors govern the precision of this 4-$\theta$ projection technique. One is the ability of Equation 2 to accurately characterise the dependency of a creep curves shape on test conditions. It may well be the case that the $\theta_{ij}$'s are related to stress and temperature in a more complex non-linear way. It is here that scope may exist for the incorporation of neural networks into the Theta projection concept. A second governing factor is the degree to which Equation 1 represents the experimental creep curve. It is well known by practitioners of this technique that although Equation 1 is a very good representation of creep curves for materials of moderate to high ductility, it gives quite a poor fit at low strains and times. This inevitably leads to difficulties in the prediction of very low strain properties using Equation 5 (such as time to 0.5% strain). But because this mis-specification is over very rapidly, it is to be expected that this has virtually no effect on creep properties such as the minimum creep rate and time to failure.

Evans [5] has recently suggested a solution to this mis-specification problem that should improve the prediction of low strain properties using the Theta projection technique. A general model function that has the same form as Equation 1 is

$$\varepsilon_t = \eta(\theta) = \sum_{i=1}^{q} \theta_{2i-1}(1 - e^{-\theta_{2i}}). \tag{6}$$

If $\theta_{2i-1} > 0$, the $i$th term in this series represents a process which has a creep rate decreasing with increasing time (e.g. a normal primary curve). If $\theta_{2i-1} < 0$ and $\theta_{2i} < 0$ the term has a rate which increases with increasing time (e.g. a tertiary process). The fit of this model to any experimental creep curve can be made as close as desired by just increasing the value of $q$. Although there is no theoretical limit to the value of $q$, each term in Equation 6 needs to be capable of a theoretical explanation in terms of micro mechanisms governing high temperature creep. Also, estimating Equation 6 when $q$ is large presents huge practical problems in terms of being able to actually estimate all the $\theta_i$ values. Correlation's between the estimated $\theta_i$ values is likely to prevent the identification of each and every $\theta_i$ value.

Primary and tertiary creep in precipitation hardened creep resisting alloys are known to be well represented by the first and second terms in Equation 1 so that agreement to experimental observation may be achieved by the inclusion of just one further term

$$\varepsilon_t = \theta_1(1 - e^{-\theta_2 t}) + \theta_3(e^{\theta_4 t} - 1) + \theta_5(1 - e^{-\theta_6 t}). \tag{7}$$

$\theta_5$ and $\theta_6$ are two additional parameters required to improve the fit of the creep curve to the experimental data over the early primary stage. Using Equation 7 gives a 6-$\theta$ projection technique, where for example, the minimum creep rate can be predicted by substituting in the extrapolated $\tilde{\theta}_{ij}$ values into

$$\frac{\theta_{1j}\theta_{2j}^2}{\theta_{3j}\theta_{4j}^2} e^{t[-\theta_{2j}-\theta_{4j}]} + \frac{\theta_{5j}\theta_{6j}^2}{\theta_{3j}\theta_{4j}^2} e^{t[-\theta_{6j}-\theta_{4j}]} - 1 = 0 \tag{8}$$

and solving numerically. Again a prediction of the time to reach some specified creep stain $\varepsilon^*$ can be obtained by solving numerically for $t$ in the equation

$$\tilde{\theta}_{1j}(1-e^{-\tilde{\theta}_{2j}t}) + \tilde{\theta}_{3j}(e^{\tilde{\theta}_{4j}t}-1) + \tilde{\theta}_{5j}(1-e^{-\tilde{\theta}_{6j}t}) - \varepsilon^* = 0. \tag{9}$$

The failure time $t_F$ can be predicted by solving Equation 9 when $\varepsilon^*$ equals the rupture strain. This will again require the rupture strain to be extrapolated to the required conditions.

## 3.2. Estimation

Estimation of the $\theta_i$ parameters in Equation 1 and Equation 7 requires the use of non-linear optimisation algorithms. These algorithms can then choose values for $\theta_i$ that either minimise the squared deviations of all the recorded strain values around the fitted creep curve or maximise the joint probability of observing all the recorded strain/time data points, i.e. maximise the so called likelihood function. If $e_t$ is used to represent the deviation of each strain value from the fitted creep curve, then Equation 7 can be expressed in stochastic form as

$$\varepsilon_t = \tilde{\theta}_1(1 - e^{-\tilde{\theta}_2 t}) + \tilde{\theta}_3(e^{\tilde{\theta}_4 t} - 1) + \tilde{\theta}_5(1 - e^{-\tilde{\theta}_6 t}) + e_t. \tag{10}$$

where $\tilde{\theta}_i$ is an estimate of $\theta_i$. These deviations arise for many reasons. One reason is the mis-specification issue addressed above where the values for $e_t$ are expected to diminish as $q$ is increased. This aside $e_t$ also results from experimental inadequacies such as deficiencies in extensometer design, transducers, and temperature control. These experimental issues also inevitably result in values for $e_t$ being correlated with previous values for $e_t$. This so called autocorrelation can be expressed in the following way

$$e_t = \rho e_{t-1} + v_t \tag{11}$$

where $\rho$ is the first order autocorrelation coefficient, $e_{t-1}$ is the previously recorded value for $e$ and $v_t$ is an additional error variable that is free of autocorrelation. If such autocorrelation is ignored when using an optimisation algorithm to estimate each $\theta_i$, then although the resulting estimates will be unbiased they will be inefficient. That is, the uncertainty or variability associated with each estimate of $\theta_i$ will be under estimated. Thus the non linear least squares approach chooses values for $\theta_i$ and $\rho$ such that $\sum_1^n v_t^2$ is minimised, where

$$\begin{aligned} v_t = \varepsilon_t - \big\{&\tilde{\theta}_1(1 - e^{-\tilde{\theta}_2 t}) + \tilde{\theta}_3(e^{\tilde{\theta}_4 t} - 1) \\ &+ \tilde{\theta}_5(1 - e^{-\tilde{\theta}_6 t})\big\} - \rho\big\{\varepsilon_{t-1} - \big[\tilde{\theta}_1(1 - e^{-\tilde{\theta}_2 t-1}) \\ &+ \tilde{\theta}_3(e^{\tilde{\theta}_4 t-1} - 1) + \tilde{\theta}_5(1 - e^{-\tilde{\theta}_6 t-1})\big]\big\} \end{aligned} \tag{12}$$

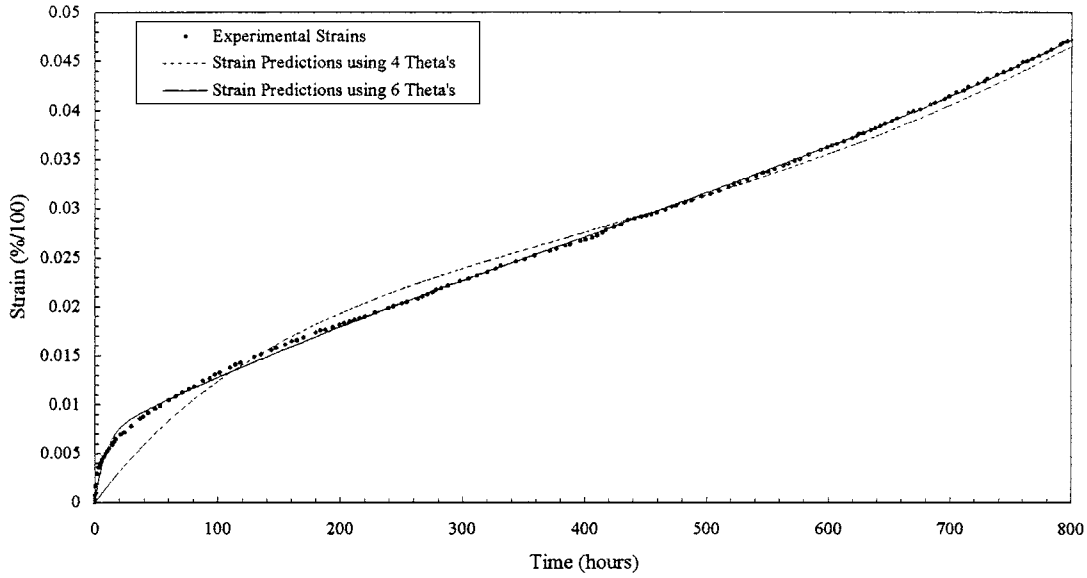


(a)

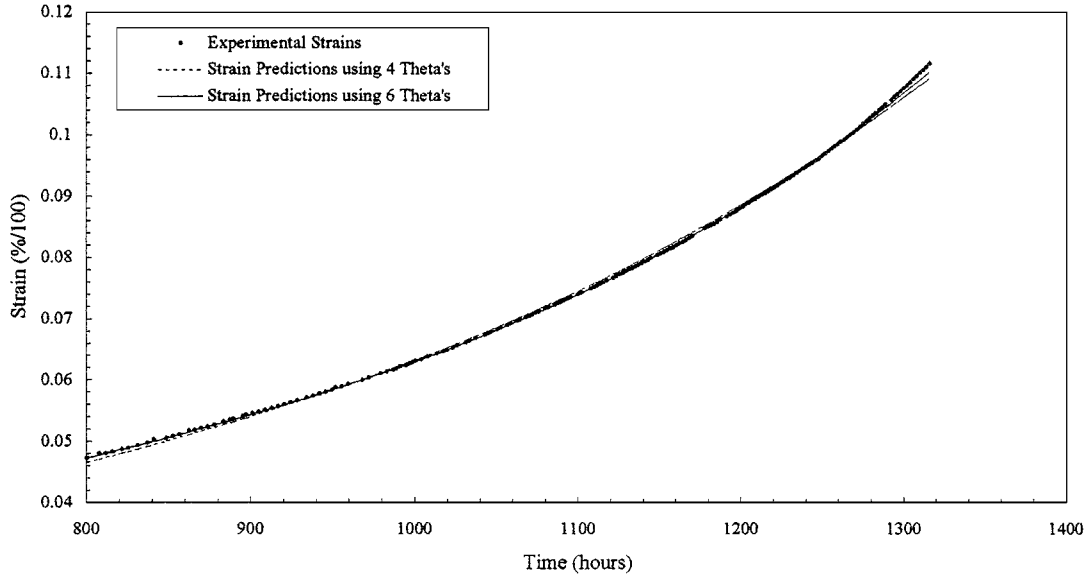


(b)

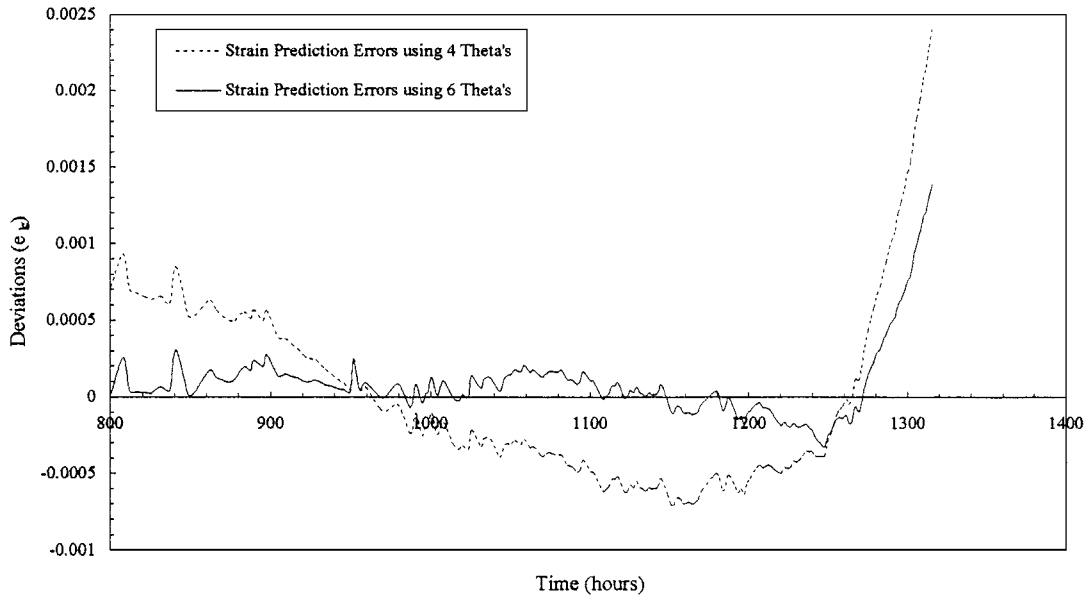


(c)

*Figure 2* (a) Comparison between experimental and predicted creep strains over the first 800 hours of testing using Equation 1 and Equation 7 at 863 K and 165 MPa. (b) Comparison between experimental and predicted creep strains over the last 600 hours of testing using Equation 1 and Equation 7 at 863 K and 165 MPa. (c) Comparison of deviations of experimental strains around Equation 1 and Equation 7 at 863 K and 165 MPa.

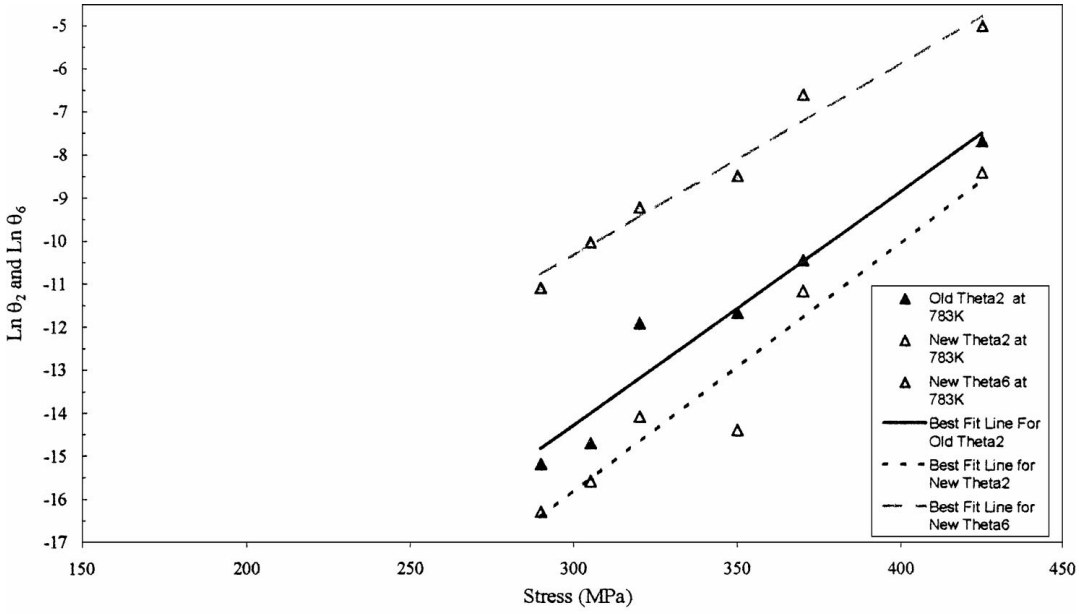


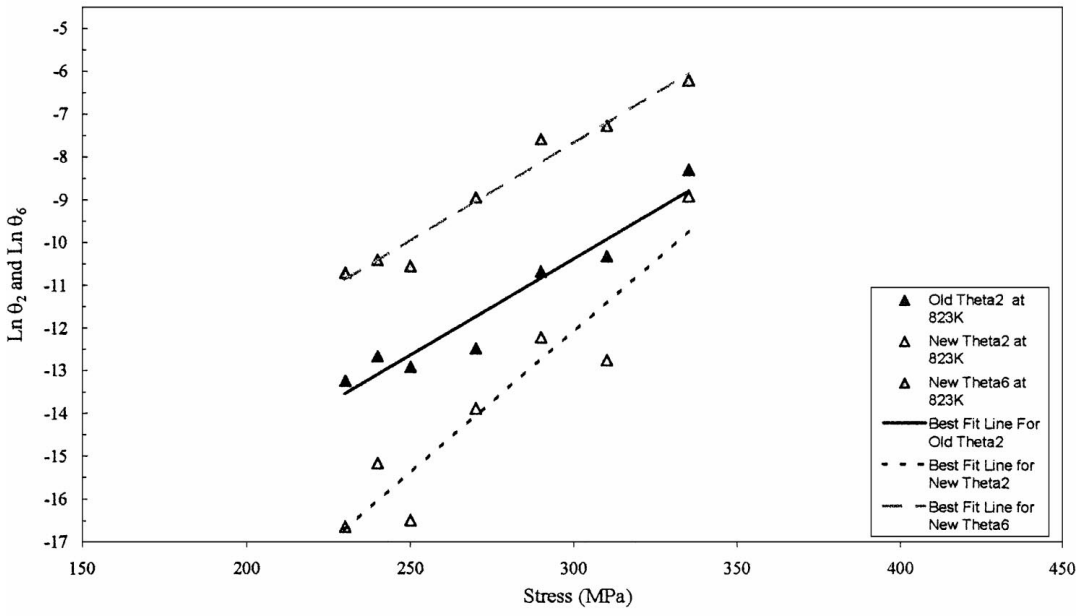


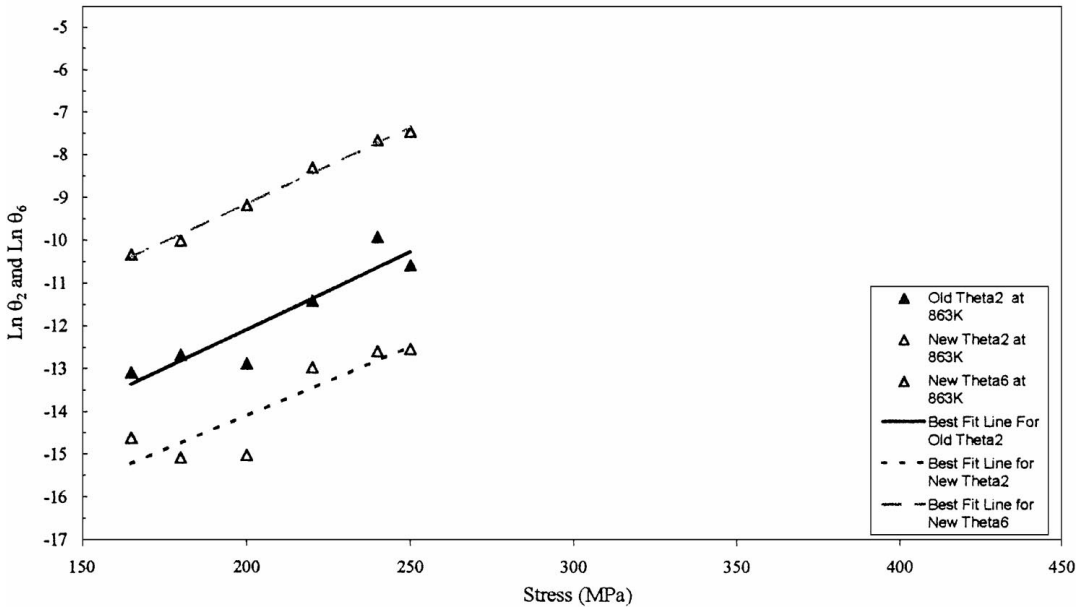


(a)

*Figure 3* (a) The variation of $\theta_2$ and $\theta_6$ with stress at 783 K, 823 K and 863 K for 1CrMoV rotor steel. (b) The variation of $\theta_4$ with stress at 783 K, 823 K and 863 K for 1CrMoV rotor steel. (c) The variation of $\theta_3$ with stress at 783 K, 823 K and 863 K for 1CrMoV rotor steel. (d) The variation of $\theta_1$ and $\theta_5$ with stress at 783 K, 823 K and 863 K for 1CrMoV rotor steel. (*Continued*)

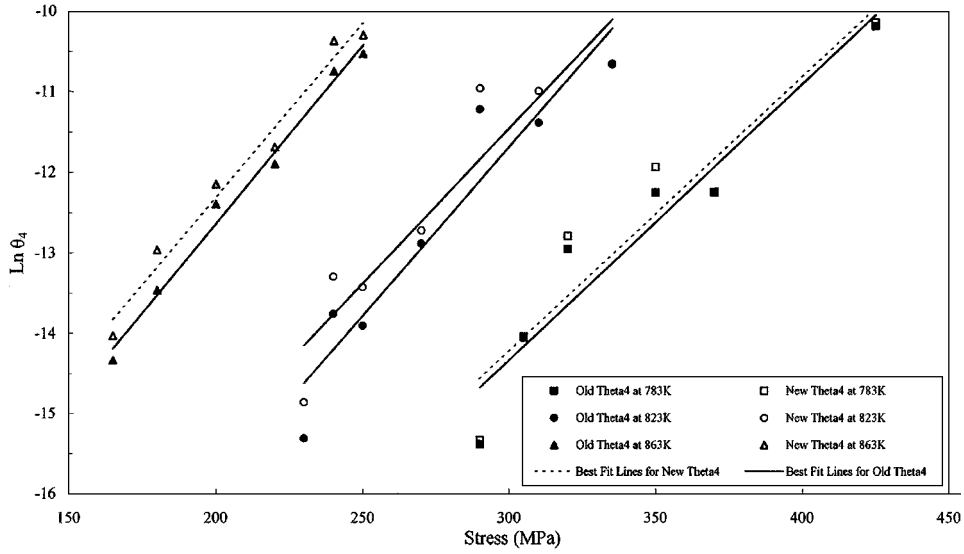


(b)

*Figure 3* (*Continued.*)

If $e_t$ is assumed to be normally distributed then the log likelihood function for $\varepsilon_t$ is of the form (see Greene [7] for more details)

$$\begin{aligned}\text{Log}(L) = &-0.9818 - \ln(s) + 0.5\ln(1-\rho^2) \\ &- \frac{1}{2s^2}\{(1-\rho^2)(\varepsilon_t - U_1)^2 \\ &+ (\varepsilon_t - U_t - \rho(\varepsilon_{t-1} - U_{t-1})^2\} \quad (13)\end{aligned}$$

where, $U_t = \tilde{\theta}_1(1-e^{-\tilde{\theta}_2 t}) + \tilde{\theta}_3(e^{\tilde{\theta}_4 t} - 1) + \tilde{\theta}_5(1-e^{-\tilde{\theta}_6 t})$, $U_1$ is the first value for $U_t$ and $s$ is standard error for $v_t$. Even when normality is assumed, the least squares and maximum likelihood techniques will only give the same estimated values for $\theta_i$ when $\rho = 0$. In the presence of autocorrelation the two techniques will give differing estimates.

Equation 13 can be maximised or $\sum_1^n v_t^2$ minimised using any standard numerical optimisation technique. This paper has made use of the *Solver* program within Excel 97. This program uses the Newton-Raphson algorithm with all central derivatives being estimated numerically. Maximum likelihood was selected over the least squares procedure usually adopted by theta practitioners because it allows for future work to generalise the distribution for $e_t$ and so obtain more reliable confidence bounds for any estimated creep curve.

Finally, there is the issue of how to estimate the values for $\beta_i$ in Equation 2. Ordinary least squares works by minimising the squared deviation between the actual $\theta_{ij}$ value and the estimated surface depicted by Equation 2. If $e'_{ij}$ represents such deviations for a given $\theta_{ij}$ then $\beta_0$ to $\beta_3$ are chosen to minimise $\sum_{j=1}^m e'^2_{ij}$. When this technique is used the resulting 4-$\theta$ and 6-$\theta$ creep property predictions are said to be unweighted. However, any value obtained for $\theta_{ij}$ is only an estimate of its true value and, depending on the nature of the data, some $\theta_{ij}$'s will be estimated with more reliability than others. This reliability is of course measured by the variance associated with each $\theta_{ij}$. This being the case it makes sense to minimise a weighted error sum of squares, $\sum_{j=1}^m (w_{ij} e'^2_{ij})$. Evans [1] has shown that the $w_{ij}$ weights should equal

$$w_{ij} = \frac{\theta_{ij}^2}{\text{Var}\{\theta_{ij}\}} \quad (14)$$

where var($\theta_{ij}$) is the variance associated with the $\theta_{ij}$ estimate. This makes sense because the larger is the estimated value for $\theta_{ij}$ relative to the uncertainty associated with this estimate, the more influence that estimate should have on the values for $\beta_i$. When this technique is used, the resulting 4-$\theta$ and 6-$\theta$ creep property predictions are said to be weighted.

## 4. Comparison of 4-$\theta$ and 6-$\theta$ estimates

In Fig. 2a the first 800 hours of the experimental creep curve obtained at 863 K and 165 MPa is shown together with the fits obtained from using Equations 1 and 7. It is immediately apparent that the equation containing six $\theta$'s is a much better descriptor of the strain data over all the times shown. This is especially true for strain values below 0.015. Fig. 2b shows that for the latter part of the creep curve both Equation 1 and Equation 7 fit equally well. This is further confirmed in Fig. 2c which shows the deviations ($e_t$ values) of the experimental strain data around the fitted creep curves (using Equation 1 and Equation 7) from initiation time to rupture time. The deviations around the equation containing six $\theta_i$'s oscillate tightly around the zero axis almost until rupture strain occurs. It is therefore to be expected that the 6-$\theta$ approach will produce better predictions than the 4-$\theta$ approach of times to low strain but similar predictions of time to rupture strain.

Fig. 3a to d give a more complete comparison of the 6-$\theta$ and 4-$\theta$ results by showing the variation of each $\theta_i$ with stress and temperature. For comparison purposes both Equation 1 and Equation 7 were estimated with the $\theta_i$ estimates from Equation 1 being labelled old Theta's and the $\theta_i$ estimates from Equation 7 the new Theta's. Fig. 3a shows the rate parameters on the primary part

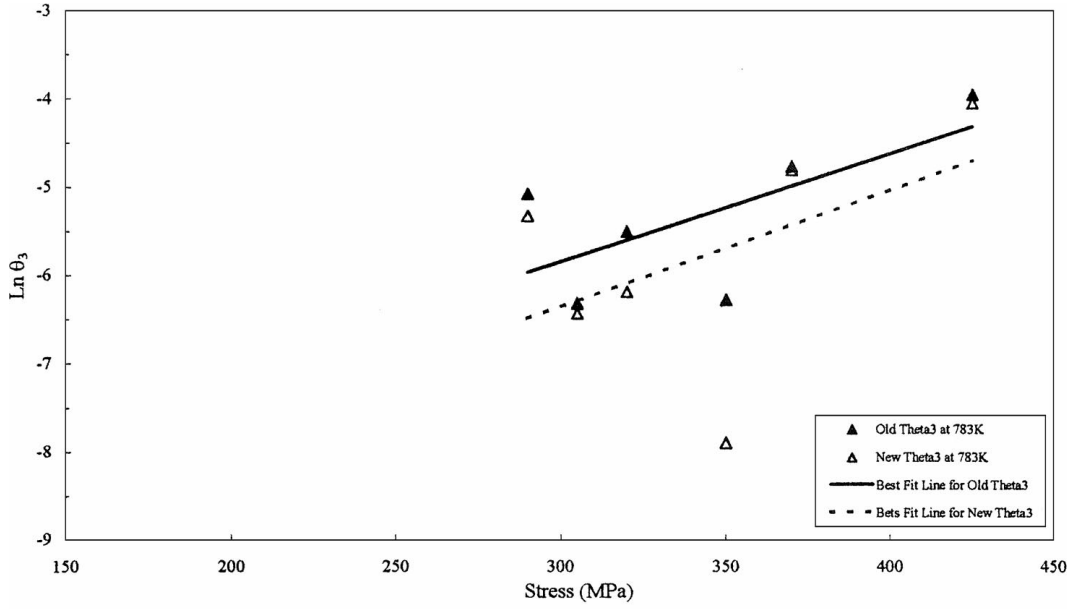


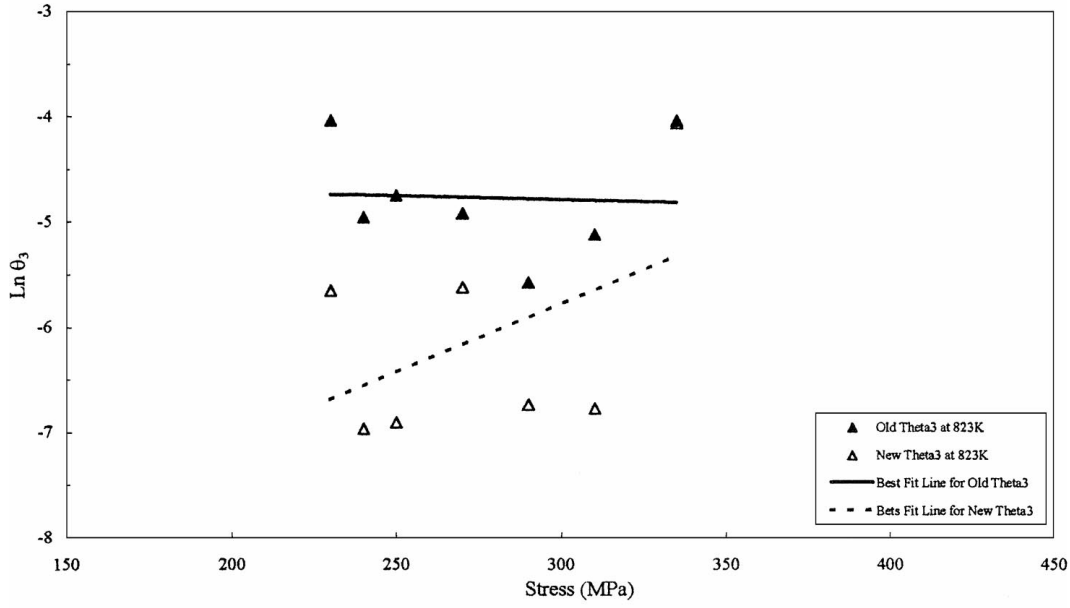


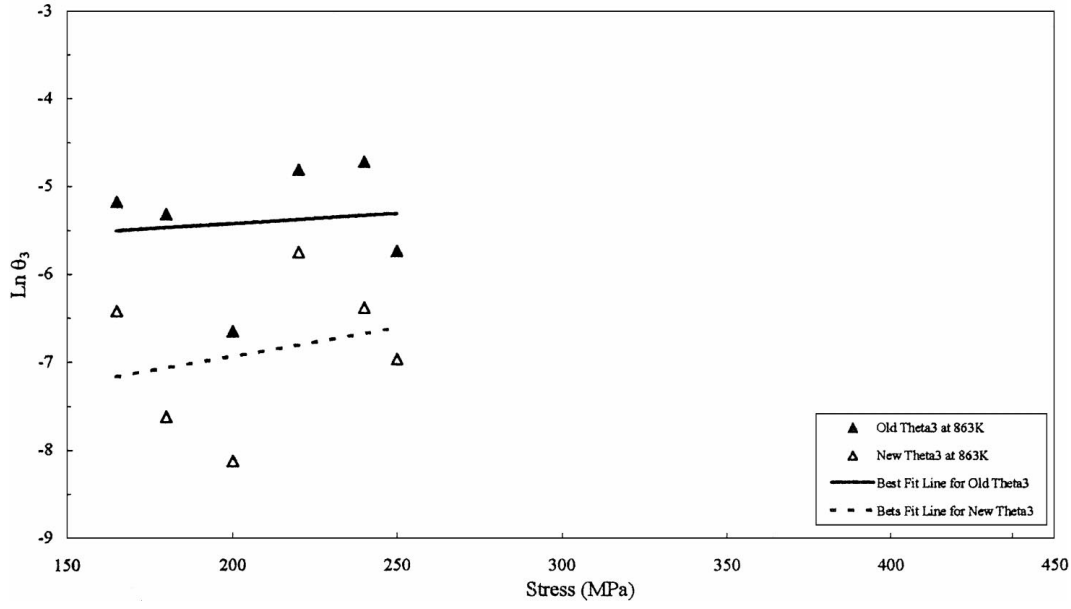


(c)

*Figure 3* (*Continued.*)

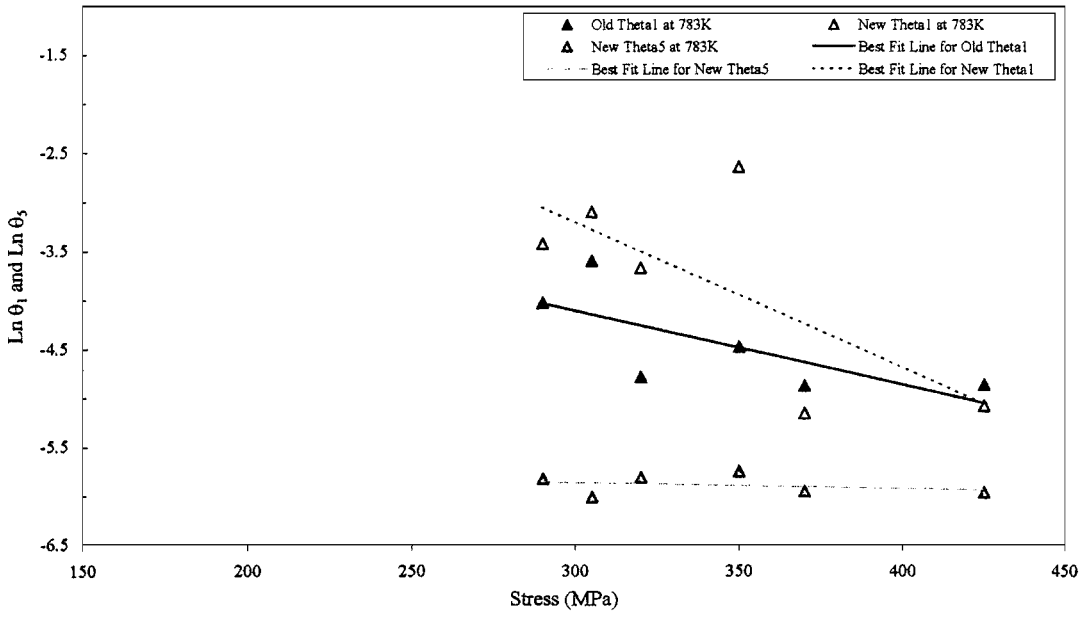


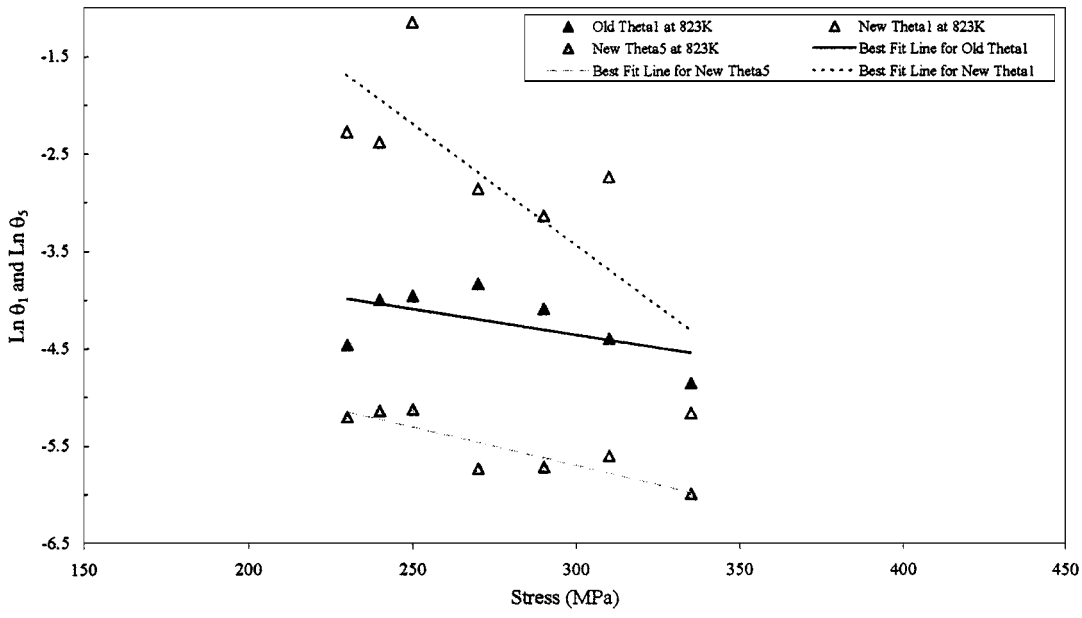


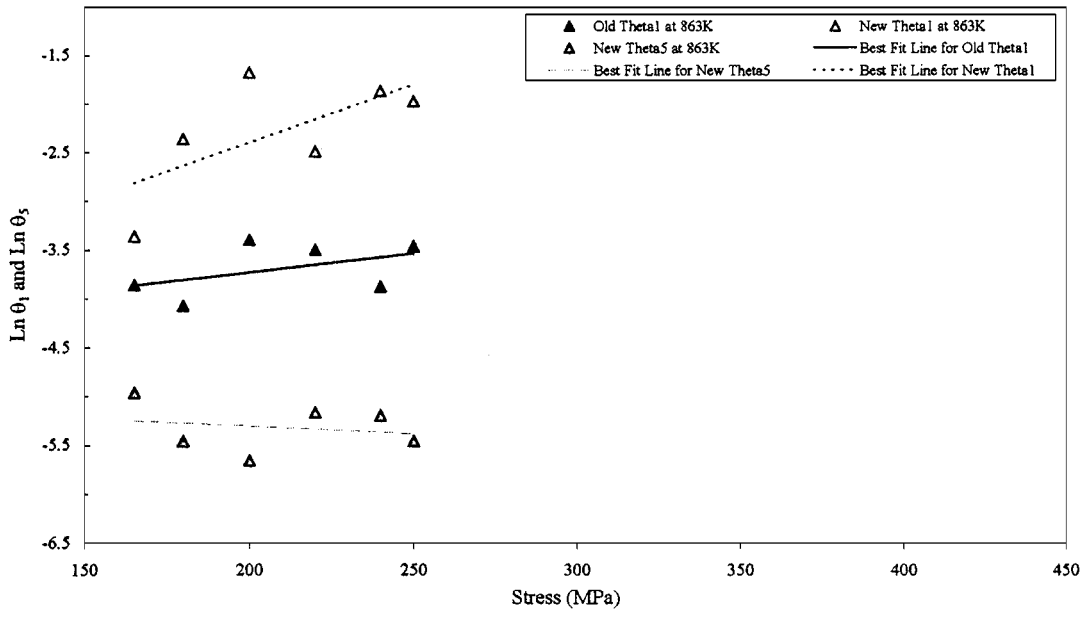


(d)

*Figure 3* (*Continued.*)

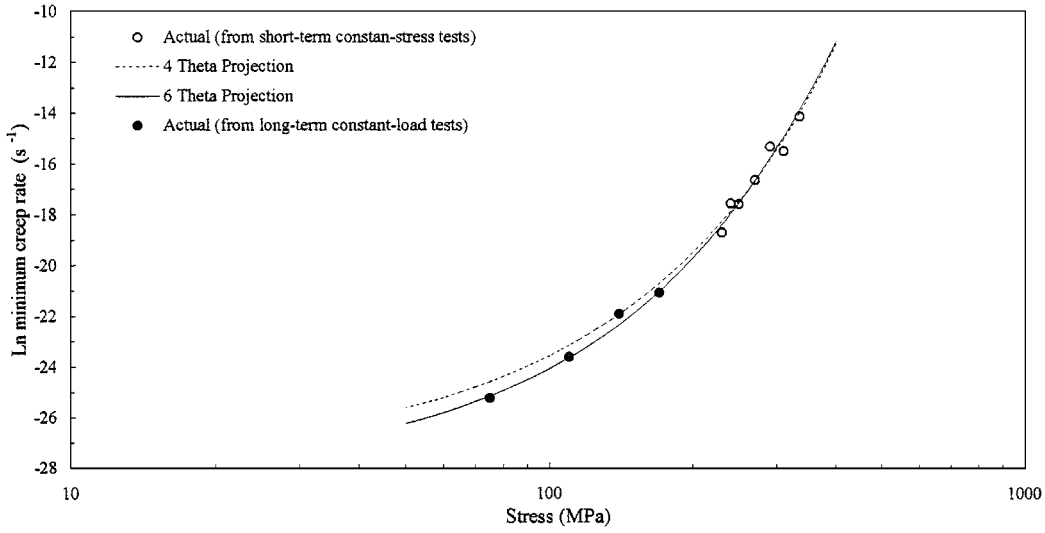


(a)

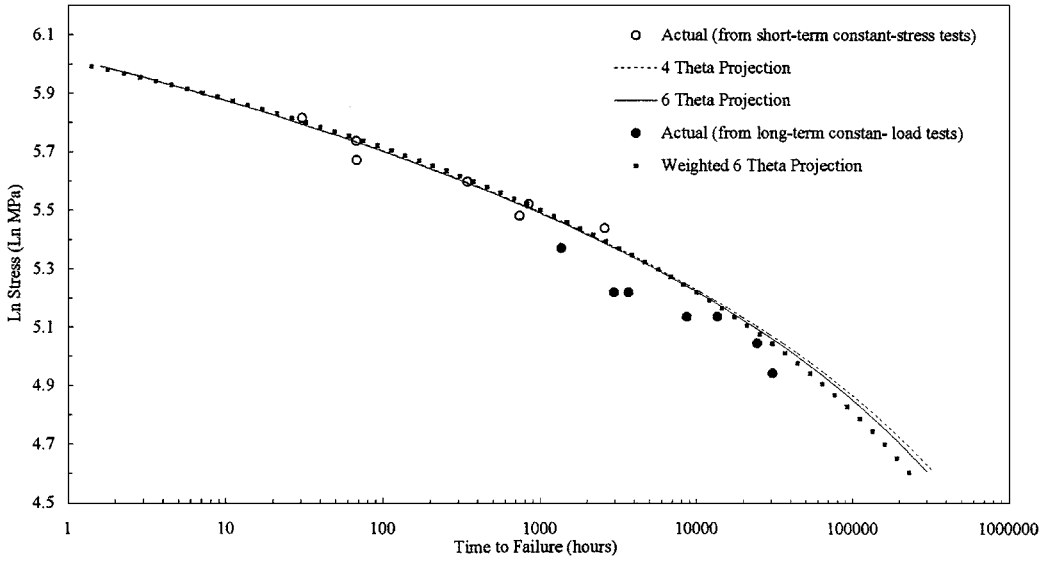


(b)

*Figure 4* (a) Constant-stress $\log\sigma/\log\varepsilon_m$ relationships predicted from the $\theta$ data for the 1CrMoV rotor steel and 823 K. The plot includes the measured $\varepsilon_m$ values obtained from the short-term constant-stress tests at 823 K, and the long-term results of the constant-load tests at 823 K. (b) Predicted $\log\sigma/\log t_F$ plots for constant stress conditions, compared with the measured $t_F$ values obtained from short-term constant-stress tests and long-term constant-load tests at 823 K.

of the creep curves. As can be seen one primary rate (old $\theta_2$) is replaced by two new ones (new $\theta_2$ and new $\theta_6$) with these new estimates being either side of the old estimates. The unweighted best fit lines superimposed around the experimental data show that the old and new theta's vary in a very similar way with stress. Further, the new estimates for $\theta_6$ seems to vary more predictably with stress that the old $\theta_2$ estimates, whilst the new $\theta_2$ estimates has more variability about the best fit line compared to the old $\theta_2$ estimates.

Fig. 3b shows the rate term on the tertiary part of the creep curves. It is very encouraging to note that the new and old estimates for $\theta_4$ are very similar and give almost identical trend line variations with stress. Consequently, it is to be expected that the rupture time predictions obtained from the 4-$\theta$ and 6-$\theta$ techniques should be broadly comparable. The advantage of the 6-$\theta$ technique then being its ability to better predict times to low strain by using the new estimates of $\theta_6$.

Fig. 3c and d show the strain like quantities from Equations 1 and 7. As reported previously for several steels [8, 9] the old strain quantities (old $\theta_1$ and old $\theta_3$) do not vary markedly with stress and temperature. The same also appears to be true for the new strain like parameters—new $\theta_1$, new $\theta_3$ and new $\theta_5$.

## 5. Comparison of 4-$\theta$ and 6-$\theta$ long term predictions

Fig. 4a shows the relationship between the natural log of the minimum creep rate and stress predicted from the unweighted 4-$\theta$ and 6-$\theta$ relationships, together with the measured short-term and long-term property values. (Weighting had little affect on the predictions). The predicted behaviour patterns agree very well with the measured long-term data, with the 6-$\theta$ relationship performing marginally better at the lower two stress readings.

Fig. 4b shows the relationship between stress and time to failure predicted from the 4-$\theta$ and 6-$\theta$ relationships, together with the measured short-term and long-term property values. Again the predicted behaviour

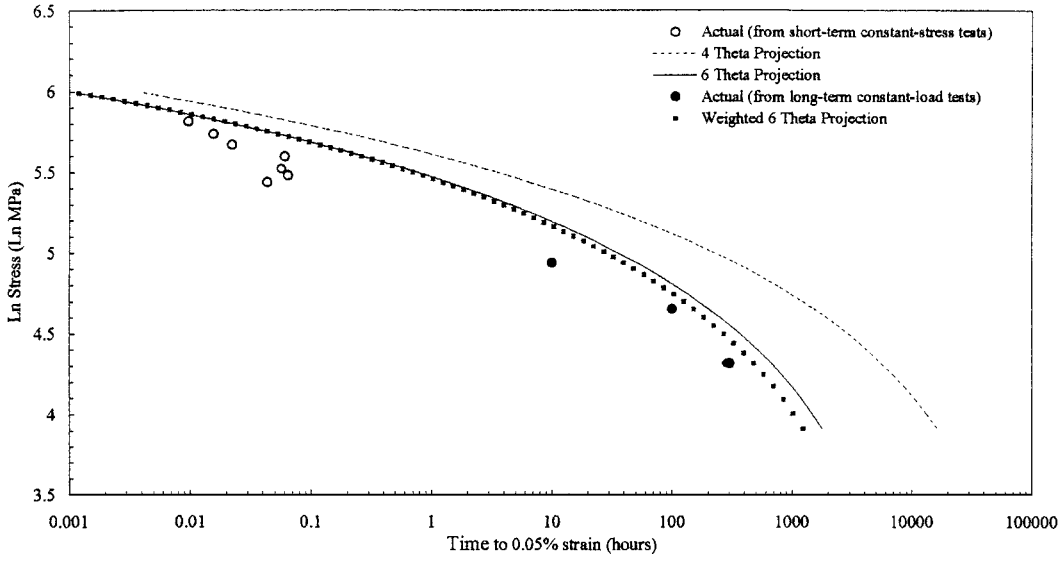


(a)

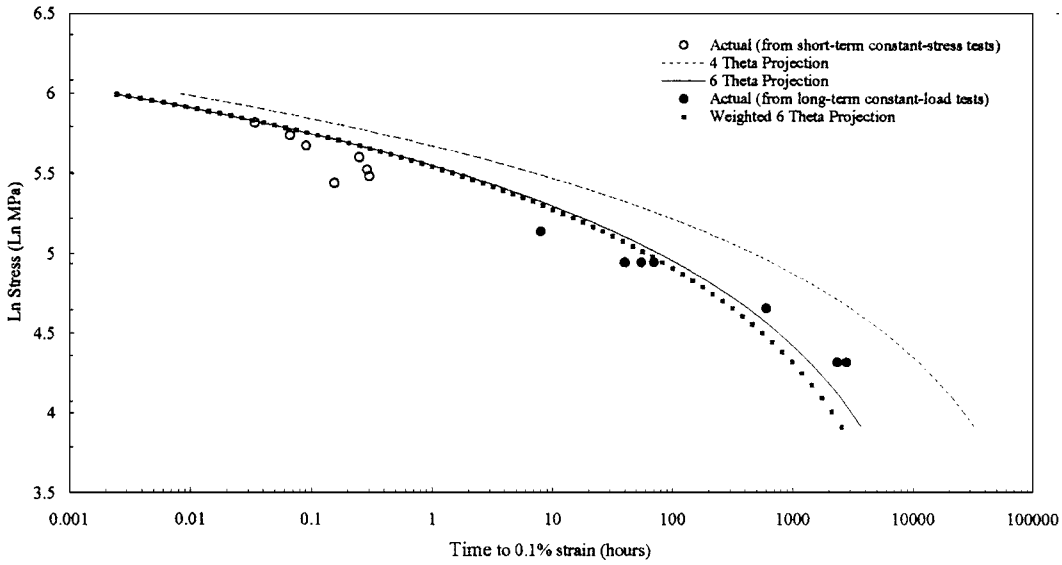


(b)

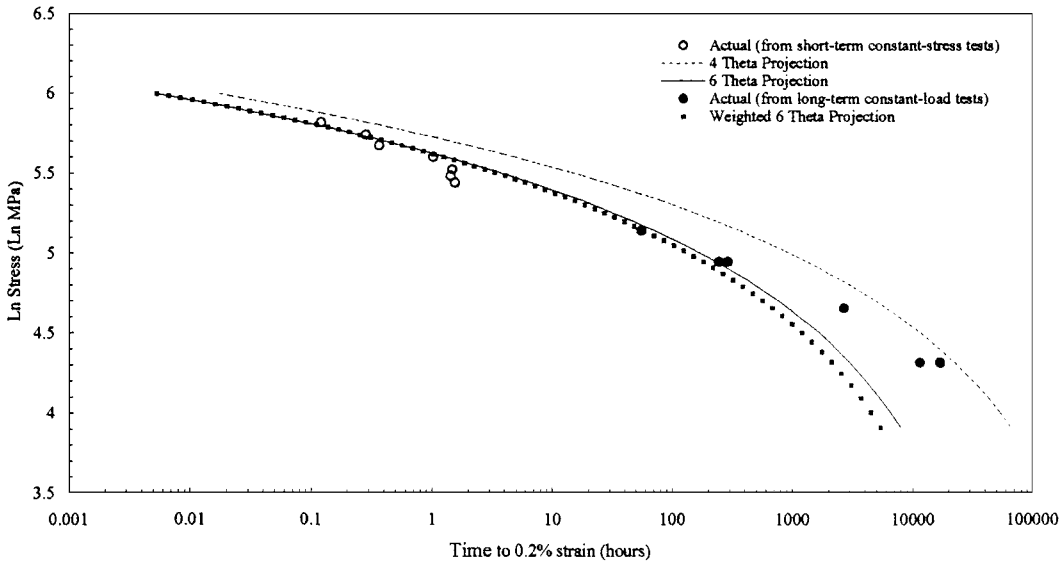


(c)

*Figure 5* (a) Predicted $\log\sigma/\log t_{0.05\%}$ plots, compared with the measured $t_{0.05\%}$ values obtained from short-term constant-stress tests and long-term constant-load tests at 823 K. (b) Predicted $\log\sigma/\log t_{0.1\%}$ plots, compared with the measured $t_{0.1\%}$ values obtained from short-term constant-stress tests and long-term constant-load tests at 823 K. (c) Predicted $\log\sigma/\log t_{0.2\%}$ plots, compared with the measured $t_{0.2\%}$ values obtained from short-term constant-stress tests and long-term constant-load tests at 823 K. (d) Predicted $\log\sigma/\log t_{0.5\%}$ plots, compared with the measured $t_{0.5\%}$ values obtained from short-term constant-stress tests and long-term constant-load tests at 823 K. (e) Predicted $\log\sigma/\log t_{1.0\%}$ plots, compared with the measured $t_{1.0\%}$ values obtained from short-term constant-stress tests and long-term constant-load tests at 823 K. (*Continued*)

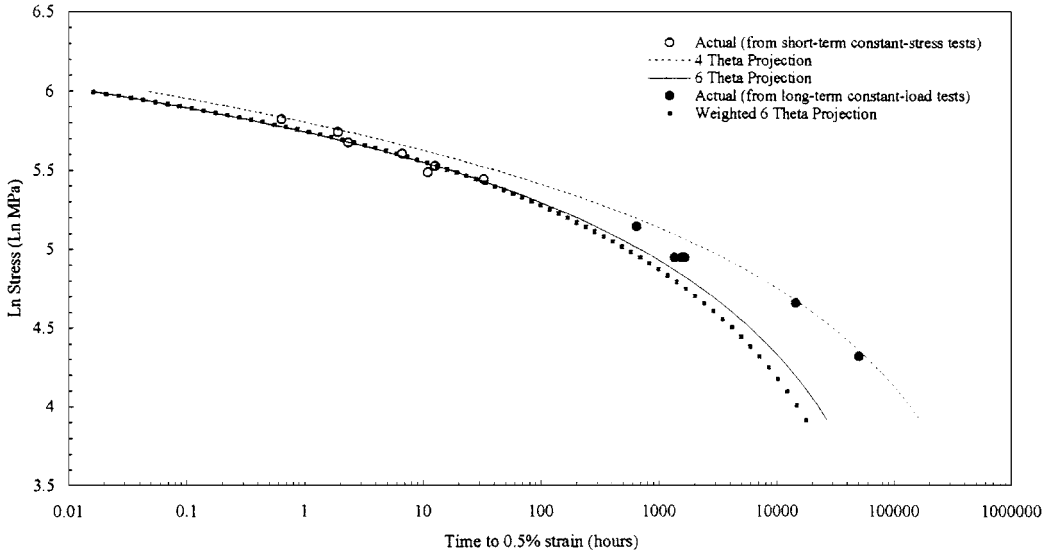


(d)

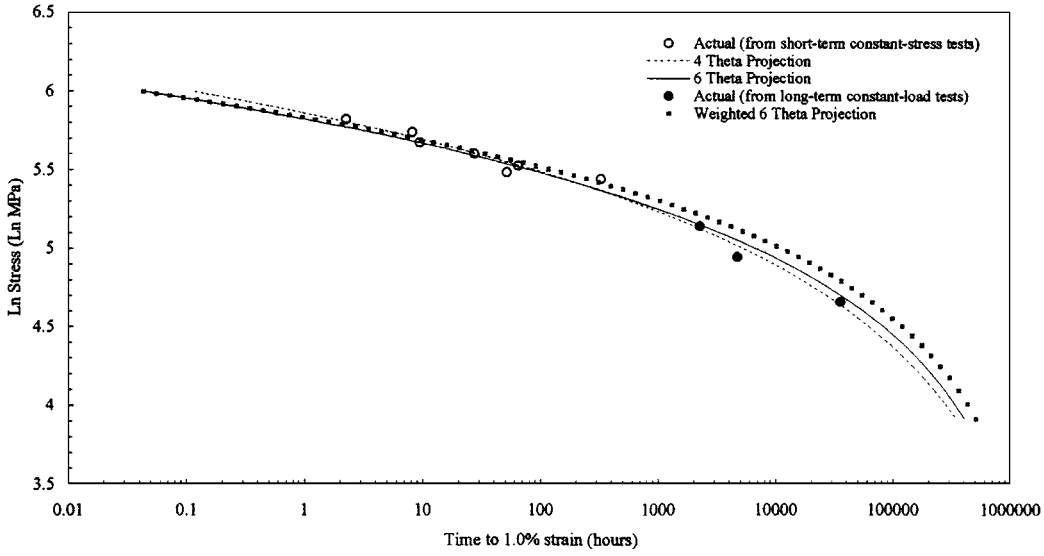


(e)

*Figure 5 Continued.*

agrees reasonably well with the measure long-term data, with the 4-$\theta$ and 6-$\theta$ predictions being almost indistinguishable. This agrees well with the expectations spelt out above. Weighting only had a visual affect on the predictions when using the 6-$\theta$ approach at very low stresses.

Fig. 5a to e shows the relationship between stress and time to various low strains predicted from the 4-$\theta$ and 6-$\theta$ relationships, together with the measured short-term and long-term property values. A number of conclusions can be drawn from these Figures. First, the 6-$\theta$ approach yields very much improved interpolations over the 4-$\theta$ approach at each and every strain shown (the predictions are closer to the short-term constant-stress test data). The interpolations obtained from the 6-$\theta$ approach also improve with increasing strain. Secondly, at very low strains (0.05% and 0.1%) the 4-$\theta$ approach is hopeless at predicting the correct long-term constant-load test data. At these strains, the 6-$\theta$ approach (in both weighted and unweighted form) produces very good long-term predictions. Curiously, at the relatively larger strains of 0.2% and 0.5%, the 4-$\theta$ approach does rather better in predicting the long-term data obtained at stresses below 140 MPa—this in spite of getting the interpolative properties completely wrong. Finally, as the strain increases the short and long-term predictions obtained from the 4-$\theta$ and 6-$\theta$ approaches tend to converge upon one another. The predictions of time to 1.0% strain, for example (see Fig. 5e), obtained using the 4-$\theta$ and 6-$\theta$ approaches are excellent and very similar. (Weighting has more of an effect on the 6-$\theta$ predictions and so weighted 4-$\theta$ predictions are not shown on these Figures.)

## 6. Conclusions

High precision constant-stress creep curves obtained for 1CrMoV rotor steel over a range of stresses at 783 K, 823 K and 863 K were analysed using the 4-$\theta$ and 6-$\theta$ projection concepts. The minimum creep rates and times to failure down to 1.0E-08 and 30,558 hours respectively were accurately predicted using both the 4-$\theta$ and 6-$\theta$ approaches, when applied to data obtained in tests with a maximum duration of 4450 hours. However, unlike the 4-$\theta$ approach, the 6-$\theta$ approach was also capable of accurately predicting times to very low strains

(0.05% and 0.1%) at stress levels as low as 77 MPa (well below the lowest stress of 230 MPa used in the theta analysis). For times to 1.0% strain or more the 4-$\theta$ and 6-$\theta$ techniques give similar short and long-term predictions.

## References


1. R. W. EVANS, *Materials Science and Technology* **5** (1989) 699.
2. R. W. EVANS, J. D. PARKER and B. WILSHIRE, in "Recent Advances in Creep and Fracture of Engineering Materials and Structures," edited by B. Wilshire and D. R. J. Owen (Pineridge Press, Swansea, 1982) p. 135.
3. F. R. LARSON and J. MILLER, in *Trans.* ASME **174**(5) (1952).
4. R. W. EVANS, M. R. WILLIS, B. WILSHIRE, S. HOLDSWORTH, B. SENIOR, A. FLEMING, M. SPINDLER and J. A. WILLIAMS, in Proceedings of the 5th International Conference on 'Creep and Fracture of Materials and Structures', Swansea, 1993, edited by B. Wilshire and R. W. Evans (The Institute of Materials, London, 1993) p. 633.
5. R. W. EVANS, *Materials Science and Technology* **16** (2000) 6–8.
6. R. W. EVANS and B. WILSHIRE, in "Creep of Metals and Alloys" (The Institute of Materials, London, 1985).
7. W. H. GREENE, in "Econometric Analysis" (Macmillan, New York, 1993) p. 430.
8. I. BEDEN, S. G. R. BROWN, R. W. EVANS and B. WILSHIRE, *Res. Mech.* **22** (1987) 45.
9. H. WOLF, M. MATHEWS, S. L. MANNAN and P. RODRIGUEZ, *Mater. Sci. Eng.* **A159** (1992) 199.



*Received 12 August*
*and accepted 10 December 1999*